Proceedings of Symposium on Ultrasonic Electronics, Vol. 35 (2014) pp. 11-12
3-5 December, 2014

# Closed-Crack Imaging and Scattering Behavior Analysis Using Confocal Subharmonic Phased Array

# 共焦点サブハーモニック超音波フェーズドアレイによる閉口き裂映像化と散乱挙動の解析

Azusa Suagawara[1‡], Kentaro Jinno[1], Yoshikazu Ohara[1] and Kazushi Yamanaka[1]
([1]Tohoku Univ.)
菅原あずさ [1‡]，神納健太郎 [1]，小原良和 [1]，山中一司 [1] ([1] 東北大)

## 1. Introduction

Accurate measurement of crack depth is required for the safety of important structures. However, ultrasound is transmitted through closed cracks. This leads to the underestimation or overlook. To solve this problem, we have developed an imaging method, subharmonic phased array for crack evaluation (SPACE)[1)] using subharmonic waves with a high temporal resolution.[2)] However, the imaging area of a single-array SPACE is limited to the vicinity of transmission focal point (TFP). It is narrow when the TFP is fixed.[3)] In this study, we develop confocal SPACE for imaging closed cracks over a wide area, and demonstrate its usefulness. Furthermore, we examine scattering behaviors depending on incident angle in experiment and in finite-difference time-domain (FDTD) simulation with a damped double node (DDN) model.[4)]

## 2. Confocal SPACE

The configuration of confocal SPACE is shown in Fig. 1. It defines multiple TFPs with multiple angles $\theta$ and distances $r$. For each TFP, the fundamental array (FA) and subharmonic array (SA) images are created based on the SPACE imaging algorithm.[3)] By merging these single focus (SF) images to a merged image, closed cracks over a wide area can be visualized. Moreover, the scattering behaviors can be observed in detail by a radar-like display that successively shows SF images with a line indicating the incident direction.

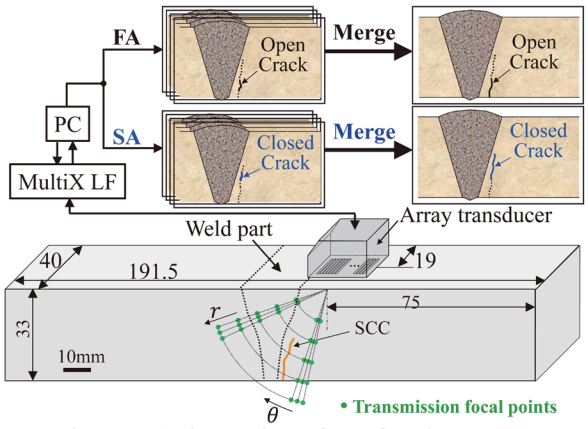


Fig. 1. Schematics of confocal SPACE.

## 3. Experimental conditions

We measured a stainless-steel (SUS304) specimen with a stress corrosion crack (SCC), which was formed in a heat affected zone in high temperature pressurized water.[3)] The experimental setup is shown in the lower part of Fig. 1. A PZT array transducer (32 elements, 5 MHz) was excited by a 3-cycle burst wave with 7 MHz and 150 V. We selected 300 TFPs with $\theta$ =12-71 ° (1 ° step) and $r$ =12-42 mm (7.5 mm step).

## 4. Experimental results

Merged images and SF images in the radar-like display for $\theta$ =50 ° and 56 ° ($r$ =27 mm) are shown in Figs. 2 and 3, respectively. Here white lines in Fig. 3 shows the incident directions. In the merged FA image (Fig. 2(a)) and the SF-FA images (Figs. 3(a) and 3(b)), many bright spots were observed which can be assigned to linear scatterings at coarse grains. In contrast, in the merged SA image (Fig. 2(b)), bright spots such as B, C and D were clearly observed. In the SF-SA images (Figs. 3(c) and 3(d)), only C was observed. These are assumed to be SCCs because these were clearly different from those in the FA images. Note that D in the merged SA image was not observed in these SF-SA images. Thus, we verified that merged SA images are nesessary for preventing underestimation.

Moreover, we found that C in Fig. 3(c) for $\theta$ =50 ° moved to the deeper position in Fig. 3(d) for $\theta$ =56 °. This is a moving crack response (MCR). It can be assumed that MCR is caused by the change in crack opening point (COP) where the crack closure stress (CCS) is equal to the tensile stress of incident wave. Thus, it was verified that radar-like display is useful for detailed analysis of scattering.

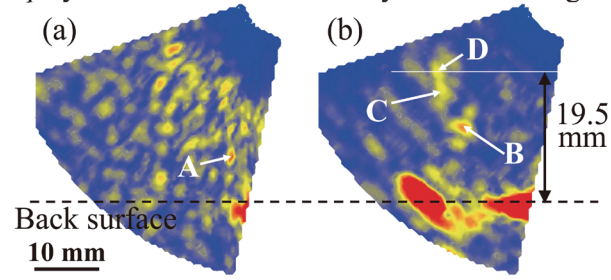


Fig. 2. Images of SCC specimen
(a)Merged FA image (b)Merged SA image.

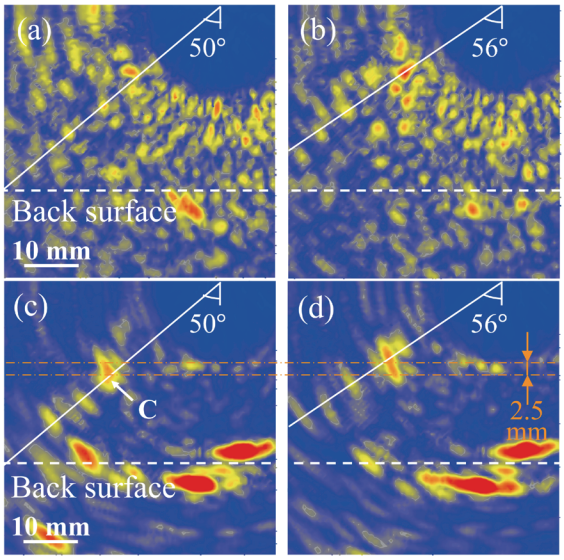


Fig. 3. SF images in the radar-like display:
(a)FA image for $\theta$ =50 ° (b) FA image for $\theta$ =56 °
(c)SA image for $\theta$ =50 ° (d) SA image for $\theta$ =56 °

## 5. Simulation conditions

To verify the assumption above, we performed an FDTD simulation. Figure 4 shows a simulation model with a vertical closed crack using the DDN model.[4,5] Gaussian-windowed 5-cycle burst waves with 7 MHz frequency and 90 nm amplitude were focused at incident angles $\theta$ =50 ° and 56 ° ($r$ = 27 mm) and were irradiated to the crack.

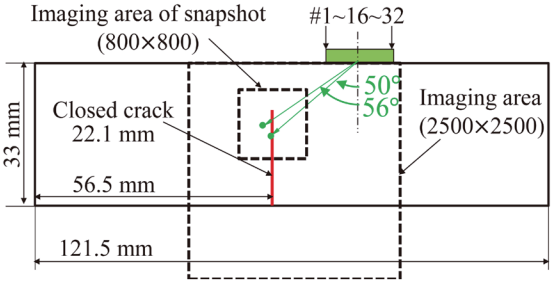


Fig. 4. Simulation model

## 6. Simulation results

The snapshots for $\theta$ =56 ° are shown in Fig. 5. The incident wave opened the crack at the COP (Fig. 5(b)). Subsequently, the lower part was opened continuously along the crack face. This behavior lasted until the tensile stress became less than the CCS at the crack closure point (CCP) (Fig. 5(c)).

Figures 6(a) and 6(b) shows simulated SA images created based on the SPACE imaging algorithm. COP and CCP were imaged, and the center of COP moved from the dashed-dotted line ($\theta$ =50 °) to the dashed-two dotted line ($\theta$ =56 °). It was also observed in snapshots that COP and CCP moved upward from $\theta$ =50 ° (Fig. 6(c)) to $\theta$ =56 ° (Fig. 6(d)). This can be due to the change in the stress distribution of the incident wave in the crack with varying $\theta$. Thus, the above analysis suggests that MCR is due to the change in COP.

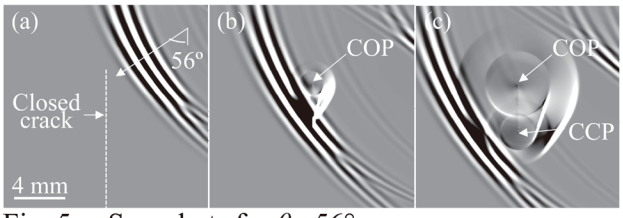


Fig. 5. Snapshots for $\theta$ =56° :
(a) $t$ =3.80 μs (b) $t$ =4.75 μs (c) $t$ =5.27 μs.

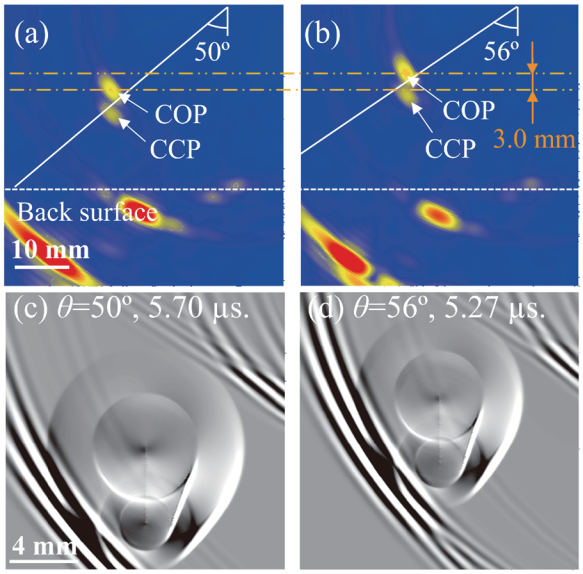


Fig. 6. Images and snapshots:
(a) SA image for $\theta$ =50° (b) SA image for $\theta$ =56°
(c) Snapshot for $\theta$ =50° at $t$ =5.70 μs
(d) Snapshot for $\theta$ =56° at $t$ =5.27 μs

## 7. Conclusion

For the measurement of closed cracks over a wide area, we have developed confocal SPACE and applied it to a closed SCC specimen. As a result, the deep SCCs were clearly imaged and accurately measured in a merged SA image, although it was underestimated in single focus SA images. Furthermore, a moving crack response (MCR) was observed with varying $\theta$ in a radar-like display. An FDTD simulation with a DDN model suggested that MCR is due to the change in the crack opening point. Thus, confocal SPACE is useful for the evaluation of structures and for the estimation of crack closure stress affecting the residual life of structures.

## References

1) Y. Ohara et al: Appl. Phys. Lett. **90** (2007) 011902.
2) K. Yamanaka et al: Jpn. J. Appl. Phys. **43** (2004) 3082.
3) Y. Ohara et al: Hihakai Kensa **60** (2011) 658 [in Japanese].
4) K. Yamanaka et al: Appl. Phys. Express **4** (2011) 076601.
5) K. Jinno et al: Mater. Trans. **55** (2014) 1017.